

Structural distortion in antiferromagnetic BaFe₂As₂ as a result of time-inversion symmetry

Ekkehard Krüger and Horst P. Strunk
*Institut für Materialwissenschaft, Materialphysik,
Universität Stuttgart, D-70569 Stuttgart, Germany*

(Dated: October 16, 2018)

As reported by Q. Huang et al. [Phys. Rev. Lett. 101, 257003 (2008)], neutron diffraction studies show an onset of antiferromagnetic order in BaFe₂As₂ associated with a tetragonal-to-orthorhombic distortion. We determine the group *Cmca* as the space group of antiferromagnetic BaFe₂As₂ and identify a roughly half-filled energy band of BaFe₂As₂ with Bloch functions of special symmetry as magnetic band. As explained by the group-theoretical nonadiabatic Heisenberg model, the electrons in this narrow band may lower their Coulomb correlation energy by producing just the experimentally observed antiferromagnetic state if this state does not violate group-theoretical principles. However, in *undistorted* BaFe₂As₂ the time-inversion symmetry of the system interferes with the stability of the antiferromagnetic state. Nevertheless, it can be stabilized by a structural distortion of BaFe₂As₂ going beyond the magnetostriction. We derive two possible structural distortions stabilizing the antiferromagnetic state. These distortions are described by their space groups and consist in mere displacements of the Fe atoms.

Keywords: magnetism, nonadiabatic Heisenberg model, group theory

I. INTRODUCTION

Neutron diffraction investigations of BaFe₂As₂ [1] revealed a tetragonal to orthorhombic distortion associated with an antiferromagnetic order where the magnetic and the structural transitions occur at the same temperature. The present paper analyses this obvious coincidence of magnetic and structural phase transitions in view of a group-theoretical approach which has already shed insight into the reasons for both magnetic and superconducting phases. This approach bases on the observation that the occurrence of a magnetic or superconducting state is always related to the existence of a narrow, almost half-filled magnetic or superconducting band of well-defined symmetry in the band structure of the respective material. Examples are the magnetic materials Cr [2], Fe [3], La₂CuO₄ [4], YBa₂Cu₃O₆ [5], and LaFeAsO [6], the (high-T_c) superconductors La₂CuO₄ [4], YBa₂Cu₃O₇, MgB₂ [7], and doped LaFeAsO [8], and numerous elemental superconductors [9, 10].

The notion of the used approach, the so-called nonadiabatic Heisenberg model, is that the electronic system in a narrow, roughly half-filled magnetic or superconducting band can lower its Coulomb correlation energy by condensing into an atomic-like state. However, for a consistent description of this atomic-like state we must also take into account the motion of the atomic cores following the electronic motion. Fortunately, we may assume that the very complex nonadiabatic localized functions representing the related localized states have the same symmetry and spin-dependence as the best localized, symmetry-adapted and, in the case of a superconducting band, spin-dependent Wannier functions of the magnetic or superconducting band. As a consequence of the special symmetry and spin-dependence of the lo-

calized states of a magnetic or superconducting band, the system is necessarily magnetic or a superconductor, respectively, in the atomic-like state [11]. In case of magnetic bands, however, an irrefutable condition is that related magnetic state does not conflict with the time-inversion symmetry of the system.

In Sec. II we shall identify the group *Cmca* (64) as the space group of the antiferromagnetic structure observed in BaFe₂As₂ (the number in parenthesis is the international number) and shall determine the magnetic group of this structure. In the following Sec. III we will verify the existence of a magnetic band related to the observed antiferromagnetic structure in the band structure of BaFe₂As₂.

In Sec. IV we shall show that this antiferromagnetic state is in fact unstable in *undistorted* BaFe₂As₂, because it conflicts with the time-inversion symmetry of the system. This statement means that the antiferromagnetic state exists in BaFe₂As₂ only, if it is accompanied by a distortion of the crystal going beyond the magnetostriction. Such distortions stabilizing an antiferromagnetic state have already been detected in La₂CuO₄ [4] and LaFeAsO [6]. In Sec. IV.2 we will determine the space groups of those distortions for BaFe₂As₂ that stabilize the observed antiferromagnetic structure.

We shall find the two possible distortions (described by their space groups) depicted in Figs. 1 (c) and (d). Both distortions can be realized by a mere displacement of the iron atoms. We tend to the distortion in Fig. 1 (c) to be most likely realized in BaFe₂As₂ because it clearly confirms the experimental observation by Huang et al. [1] that the *a* and *b* axes (denoted here in Fig. 1 (b) by *a_H* and *b_H*, respectively) have different lengths in the antiferromagnetic phase. Furthermore, this distortion is realized by nearest-neighbor Fe atoms that are oppositely displaced. Thus, the displacements are effected by a nearest-neighbor interaction between the Fe atoms

which may be more efficient than an interaction between the Fe atoms in different layers as it appears to be effective in Fig. 1 (d).

The nonadiabatic Heisenberg model does not distinguish between orbital and spin moments. Therefore, we always speak of “magnetic moments” which may consist of both orbital and spin moments.

II. THE MAGNETIC GROUP OF THE EXPERIMENTALLY OBSERVED MAGNETIC STRUCTURE

Fig. 1 (a) shows the two Fe atoms in the paramagnetic and Fig. 1 (b) the four Fe atoms in the antiferromagnetic unit cell of BaFe_2As_2 . By inspection we may recognize that Fig. 1 (b) displays the experimentally determined [1] antiferromagnetic structure because by application of the given basic translations $\mathbf{T}_1, \mathbf{T}_2, \mathbf{T}_3$ to the four Fe atoms in the unit cell we obtain just the magnetic structure presented in Fig. 3 of Ref. [1].

Removing from the space group $I4/mmm$ of BaFe_2As_2 all the symmetry operations not leaving invariant the magnetic moments of the Fe atoms [as depicted in Fig. 1 (b)], we obtain the group $Cmca = \Gamma_o^b D_{2h}^{18}$ (64) as the space group of the antiferromagnetic structure in undistorted BaFe_2As_2 . This may be proved using Figs. 1 (a) and (b) and also the “generating elements”

$$\{C_{2b}|\frac{1}{2}\frac{1}{2}\frac{1}{2}\}, \{C_{2a}|\frac{1}{2}\frac{1}{2}\frac{1}{2}\}, \text{ and } \{I|000\} \quad (1)$$

of $Cmca$, as it was detailed in Sec. 3.1 of Ref [6]. The generating elements are taken from Table 3.7 of Ref. [12], however, they are written in this paper in the coordinate system defined by Fig. 1 (b), cf. the notes to Table A.4.

Furthermore, by inspection of Fig. 1 (b) we see that the antiferromagnetic structure in undistorted BaFe_2As_2 is invariant under the anti-unitary operation $\{K|\frac{1}{2}\frac{1}{2}\frac{1}{2}\}$, where K denotes the operator of time inversion reversing all the magnetic moments and leaving invariant the positions of the atoms. Thus, the magnetic group M_{64} of the experimentally determined magnetic structure in undistorted BaFe_2As_2 may be written as

$$M_{64} = Cmca + \{K|\frac{1}{2}\frac{1}{2}\frac{1}{2}\}Cmca. \quad (2)$$

III. MAGNETIC BAND OF BaFe_2As_2

In this section we show that in the band structure of paramagnetic BaFe_2As_2 we find a magnetic band [11] related to the magnetic group M_{64} determined in the preceding section.

The band structure of paramagnetic BaFe_2As_2 (with the space group $I4/mmm$) is depicted in Fig. 2. There are Bloch functions near the Fermi level characterized by the representations

$$\Gamma_5^+, \Gamma_3^+; Z_5^-, Z_4^-; X_1^-, X_3^+, X_4^-, X_4^+; N_1^+, N_2^- \quad (3)$$

Folding the band structure into the Brillouin zone of the space group $Cmca$ of the antiferromagnetic structure in the undistorted crystal [depicted in Fig. 1 (b)], the representations (3) of the Bloch functions transform as

$$\begin{aligned} \Gamma_5^+ &\rightarrow \Gamma_2^+ + \underline{\Gamma_3^+} & \Gamma_3^+ &\rightarrow \underline{\Gamma_4^+} \\ Z_5^- &\rightarrow Y_2^- + \underline{Y_3^-} & Z_4^- &\rightarrow \underline{Y_4^-} \\ X_1^- &\rightarrow \underline{\Gamma_4^-} & X_3^+ &\rightarrow \underline{Y_4^+} \\ X_4^- &\rightarrow \underline{\Gamma_3^-} & X_4^+ &\rightarrow \underline{Y_3^+} \\ N_1^+ &\rightarrow \underline{R_1^-} + \underline{R_2^-} & N_2^- &\rightarrow \underline{R_1^+} + \underline{R_2^+} \end{aligned} \quad (4)$$

see Table A.5. The underlined representations form a magnetic band listed in Table A.7, namely band 2. The representations $Z_1 + Z_2$ as well as $T_1 + T_2$ are absent in (4) though they belong to the magnetic band, too. They may be determined by the compatibility relations given in Table A.3 and by Table A.5.

The run of the magnetic band may not be visualized until the paramagnetic band structure is folded into the Brillouin zone of the antiferromagnetic structure lying diagonally within the Brillouin zone for the paramagnetic phase. Always two lines in the paramagnetic Brillouin zone are equivalent to one line in the antiferromagnetic Brillouin zone, see Table A.1. The folded band structure with the magnetic band (highlighted by the bold line) is depicted in Fig. 3.

The Bloch functions of the magnetic band can be unitarily transformed into Wannier functions that are

- as well localized as possible,
- centered at the Fe atoms,
- and symmetry-adapted to the magnetic group M_{64} in Eq. (2),

see the notes to Table A.7.

The magnetic band in BaFe_2As_2 is roughly half-filled and extremely narrow as compared with the other bands in the band structure of this material. Thus, this band provides optimal features enabling the electrons to lower their Coulomb correlation energy [2, 3, 6, 11] by activating an exchange mechanism producing the experimentally determined antiferromagnetic structure. However, we shall show in the following Sec. IV that in *undistorted* BaFe_2As_2 this mechanism is blocked by the time-inversion symmetry of the system.

IV. STABILITY OF THE ANTIFERROMAGNETIC STRUCTURE

In this section we show that the antiferromagnetic state with the space group $Cmca$ requires a (slight) distortion of BaFe_2As_2 to form a different space group with restored time-inversion symmetry.

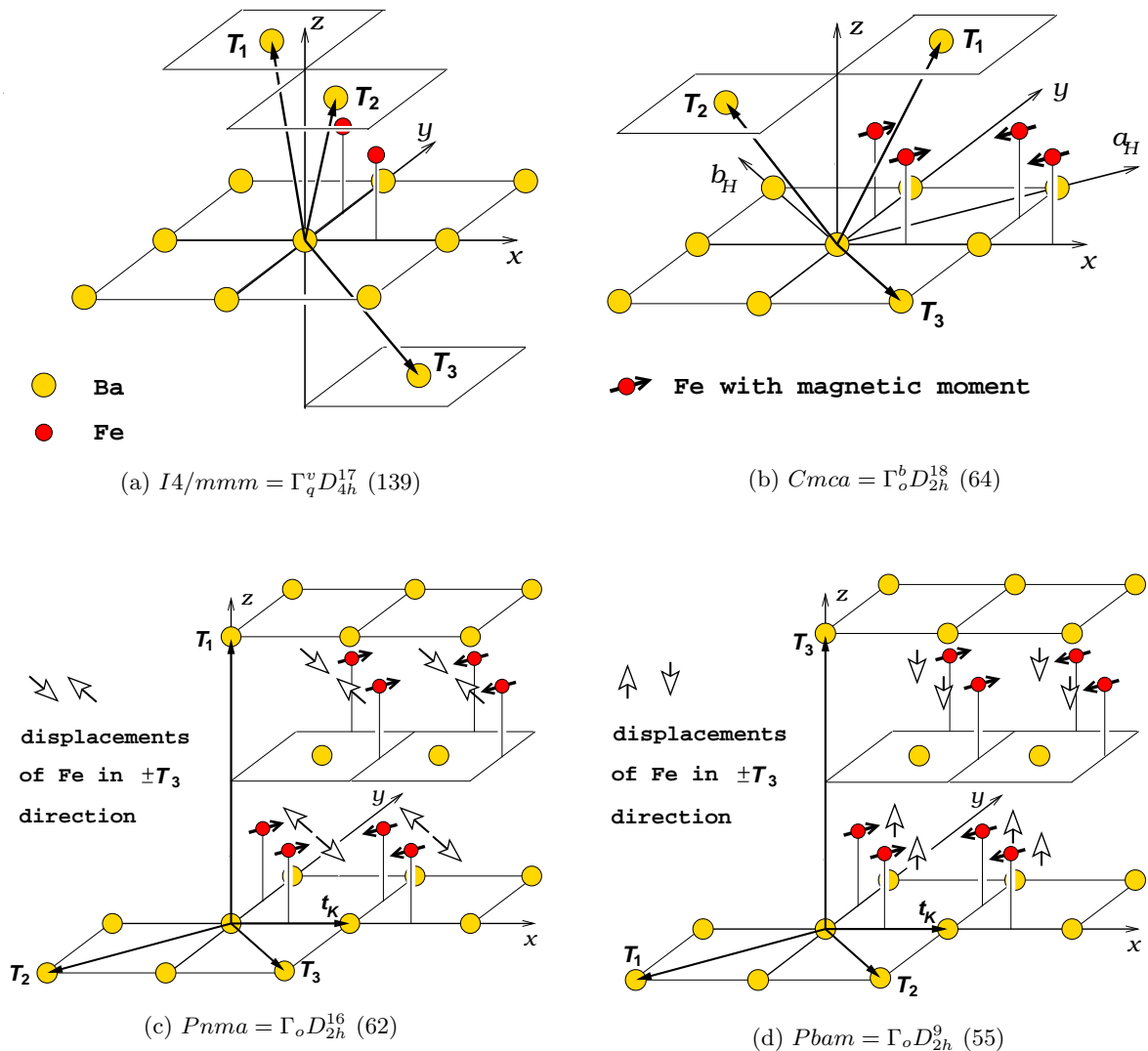


FIG. 1. Paramagnetic (a), undistorted antiferromagnetic (b) BaFe_2As_2 , and structural distortions (c) and (d) stabilizing the antiferromagnetic structure. Great (yellow) circles represent the Ba, small (red) circles the Fe atoms. For reasons of clarity the As atoms are not shown. While sufficient Ba atoms are depicted to recognize the orientation of the crystal, the Fe atoms are shown only within one unit cell. In order to facilitate a comparison of the instructive Fig. 3 of Ref. [1] with our figures, we have denoted in Fig. (b) by a_H and b_H the directions of the a and b axis used in Ref. [1]. The coordinate systems define the symmetry operations $\{R|pqr\}$ as used in this paper. They are written in the Seitz notation detailed in the textbook of Bradley and Cracknell [12]: R stands for a point group operation and pqr denotes the subsequent translation \mathbf{t} . The point group operation is related to the x, y, z coordinate system (as described in Fig. 2 of Ref. [6]), and pqr stands for the translation $\mathbf{t} = p\mathbf{T}_1 + q\mathbf{T}_2 + r\mathbf{T}_3$. While the orientation of the crystal and the x, y, z coordinate system are fixed, the basic translations \mathbf{T}_i are different in each structure. The distortions (c) and (d) may be realized by the depicted (slight) displacements of the Fe atoms in exact $\pm\mathbf{T}_3$ direction in each case [where the basic translations \mathbf{T}_3 are different in (c) and (d)]. It should be noted that the given displacements of the Fe atoms may be accompanied by additional displacements of the As or Ba atoms consistent with the respective magnetic group. The translation \mathbf{t}_K denotes the translation associated with the time inversion K . \mathbf{t}_K is a translation of the paramagnetic crystal that connects two Fe atoms with antiparallel magnetic moments and the same displacement.

IV.1. The antiferromagnetic structure is not stable in undistorted BaFe_2As_2

Assume that the magnetic state $|G\rangle$ is an eigenstate of a Hamiltonian \tilde{H} commuting with the operator K of

time inversion,

$$[\tilde{H}, K] = 0, \quad (5)$$

as it is the case within the nonadiabatic Heisenberg model, see Sec. III.C. of Ref. [2]. Nevertheless, we get

Energy (eV)

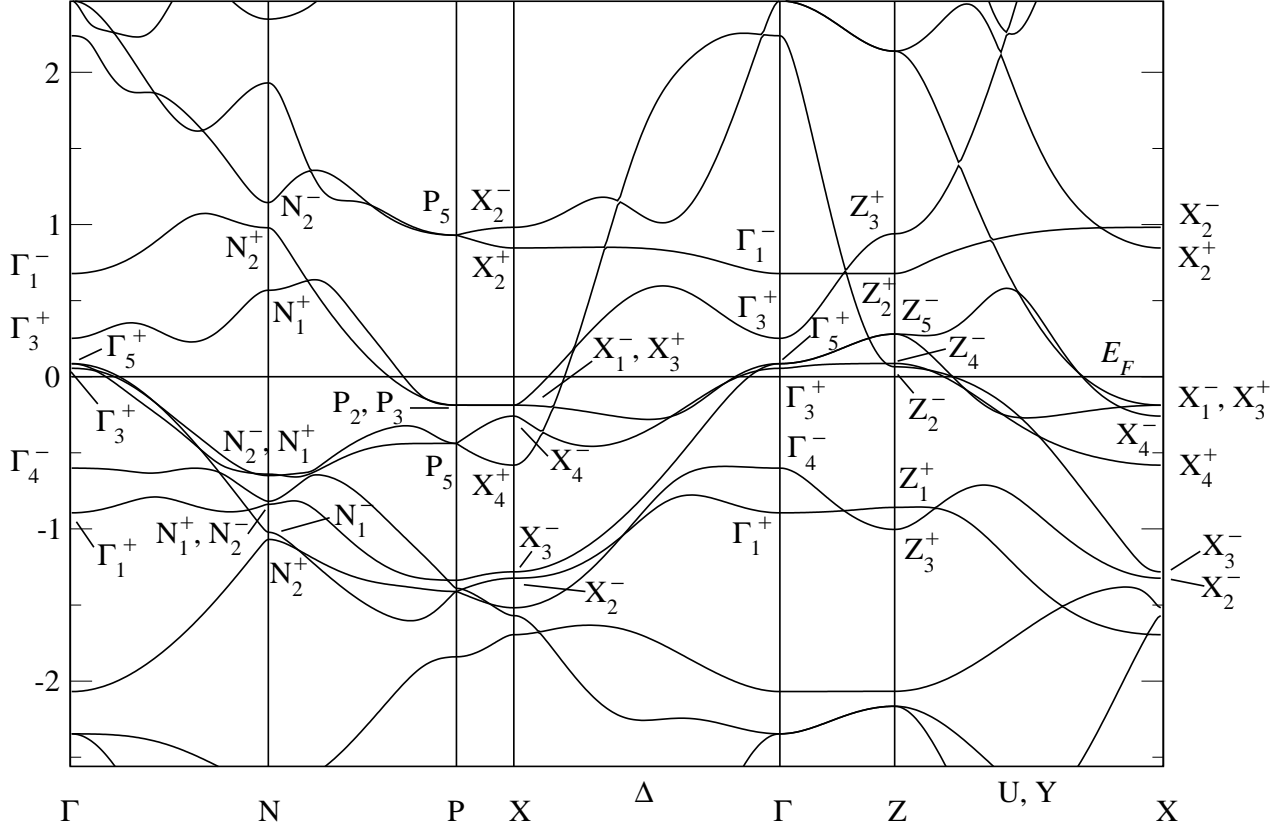


FIG. 2. Band structure of tetragonal BaFe_2As_2 as calculated by the FHI-aims program [13, 14], using the structure parameters given in Ref. [1], with symmetry labels determined by the authors. The notations of the points and lines of symmetry in the Brillouin zone for Γ_q^v follow Fig. 3.10. (b) of Ref. [12], and the symmetry labels are defined by Table A.2.

a state different from $|G\rangle$ when we apply K to $|G\rangle$,

$$K|G\rangle \neq |G\rangle, \quad (6)$$

since K reverses the magnetic moments. Consequently [2], $|G\rangle$ and $K|G\rangle$ are basis functions of a two-dimensional *irreducible* corepresentations \tilde{D} of the magnetic group \tilde{M} of \tilde{H} . \tilde{M} may be written as

$$\tilde{M} = M + KM, \quad (7)$$

where M denotes the magnetic group

$$M = S + \{K|\mathbf{t}_K\}S \quad (8)$$

of the magnetic state and S is the related space group.

However, when we restrict the symmetry operations to the subgroup M of \tilde{M} , then \tilde{D} must subduce two *one-dimensional* corepresentation D of M , because, e.g., we have

$$\{K|\mathbf{t}_K\}|G\rangle = c \cdot |G\rangle, \quad (9)$$

since the anti-unitary operator $\{K|\mathbf{t}_K\}$ belongs to the magnetic group M of the magnetic state. c is a complex number with $|c| = 1$.

If the magnetic group \tilde{M} does not possess such suitable corepresentations \tilde{D} , the related magnetic state is necessarily unstable. Fortunately, we may recognize *by the known representations of the space group S alone* whether or not \tilde{M} possesses corepresentations \tilde{D} allowing a stable magnetic state. This may be carried out by means of Theorem 4.1 in Ref. [6] reading as follows:

Theorem 1. *The magnetic group \tilde{M} (7) possesses corepresentations allowing a stable magnetic state with the space group S if S has at least one one-dimensional single-valued representation*

- (i) following case (a) with respect to the magnetic group $S + \{K|\mathbf{t}_K\}S$ (8) of the magnetic state and
- (ii) following case (c) with respect to the magnetic group $S + KS$.

The cases (a) and (c) are defined by Eqs. (7.3.45) and (7.3.47), respectively, of Ref. [12], and are given for the representations relevant in this paper in Tables A.4, A.8, and A.9. This theorem led already to an understanding of the symmetry of the incommensurate spin-density-wave states in Cr [2].

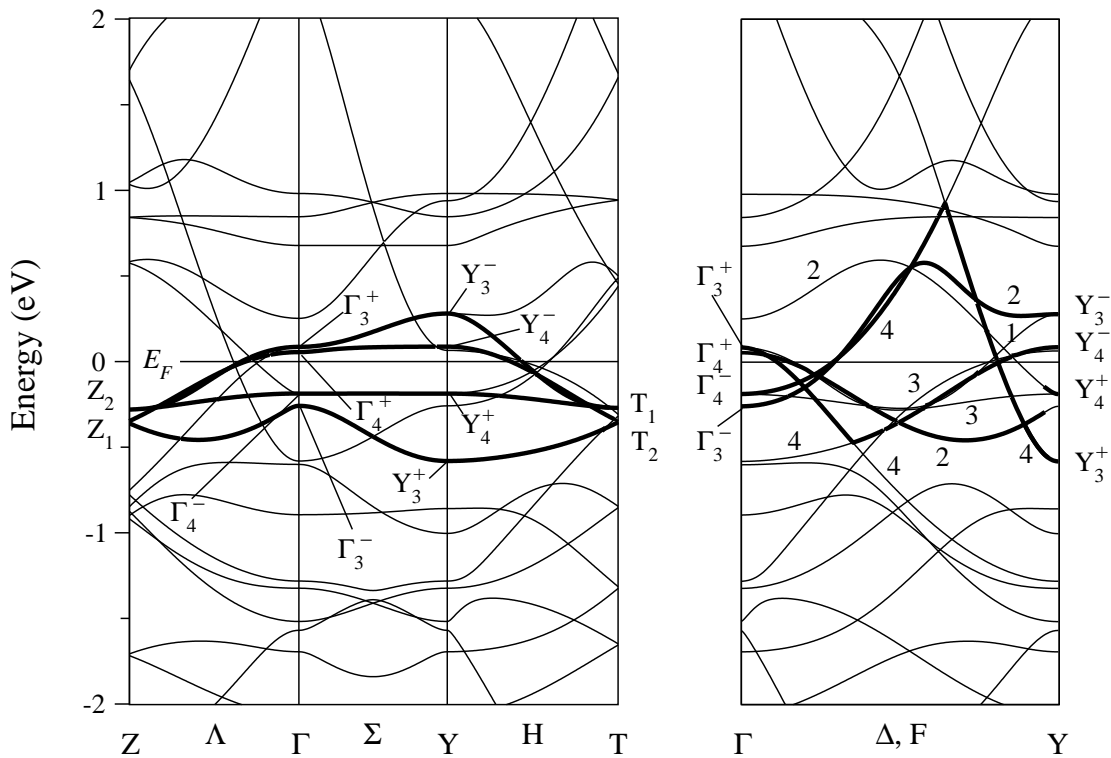


FIG. 3. The band structure of tetragonal BaFe_2As_2 (as given in Fig. 2) folded into the Brillouin zone for the Bravais lattice Γ_o^b of the space group $Cmca$ of the antiferromagnetic structure. The bold line shows the magnetic band consisting of four branches with symmetry labels that can be identified from Table A.4. The notations of the points and lines of symmetry follow Fig. 3.6 (a) of Ref. [12]. The numbers labeling the branches at the line Δ, F characterize the related representations; for instance, the number 2 stands for Δ_2 and F_2 (as defined in Table A.6). In the surroundings of the sharp peaks at the line Δ, F (between Γ and $Y(\frac{1}{2}\frac{1}{2}0)$), the Wannier functions are build from Bloch-like functions (equation (1.4) of Ref. [11]) of Δ_4, F_4 symmetry that are linear combinations of two Δ_4, F_4 Bloch functions arising from different lines in the Brillouin zone for the paramagnetic lattice Γ_q^+ . These linear combinations smooth away the peaks. Alike, the little jump between two $\Delta_2 (F_2)$ branches near Y_4^+ is bridged by a linear combination of the related $\Delta_2 (F_2)$ Bloch functions. Thus, this little jump is physically meaningless since it does not cross the Fermi level.

At first sight, the representations at point R in the Brillouin for $Cmca$ appear to comply with both conditions (i) and (ii), see Table A.4. However, not all the space group operations of $Cmca$ are comprised within the little group at R , and, consequently, the magnetic group \tilde{M} (7) related to $M = M_{64}$ (2) does not possess corepresentations allowing a stable antiferromagnetic state with the space group $Cmca$.

IV.2. Reaching stability of the antiferromagnetic state by slight distortion of the BaFe_2As_2 structure

The experimentally observed antiferromagnetic structure may be stabilized by a (small) distortion of the crystal that turns the space group $Cmca$ into an “allowed” subgroup of $Cmca$ possessing representations that allow the formation of a stable antiferromagnetic structure. In this context we considered all the space groups

- (i) leaving invariant the experimentally observed magnetic structure depicted in Fig. 1 (b) and

- (ii) meeting the two conditions in Theorem 1.

In this way we found numerous allowed space groups in antiferromagnetic BaFe_2As_2 , among them also groups containing very few symmetry operations. In the following we only consider the space groups $Pnma$ (62) and $Pbam$ (55) which are the allowed space groups of highest symmetry in antiferromagnetic BaFe_2As_2 . Both groups have the orthorhombic-primitive Bravais lattice Γ_o and comprise the full orthorhombic point group D_{2h} .

The space groups $Pnma$ and $Pbam$ can be defined by the generating elements

$$\{C_{2a}|0\frac{1}{2}\frac{1}{2}\}, \{C_{2z}|\frac{1}{2}\frac{1}{2}0\}, \{I|\frac{1}{2}\frac{1}{2}0\}, \quad (10)$$

and

$$\{C_{2a}|\frac{1}{2}\frac{1}{2}0\}, \{C_{2z}|000\}, \{I|000\}, \quad (11)$$

respectively, as given in Table 3.7 of Ref. [12]. Here, however, they are written in the coordinate systems given by Figs. 1 (c) and (d), respectively.

The symmetry operations of both $Pnma$ and $Pbam$ leave invariant the atoms of BaFe_2As_2 and the antiferromagnetic structure depicted in Fig. 1 (b). This may be

proved starting from the generating elements of $Pnma$ and $Pbam$, as it was detailed in Sec. 5.1 of Ref [6].

In contrast to the group $Cmca$, both groups $Pnma$ and $Pbam$ possess one-dimensional representations satisfying both conditions (i) and (ii) of Theorem 1. These are the representations at point U in the Brillouin zone for $Pnma$ and at points S and R in the Brillouin zone for $Pbam$, see Tables A.8 and A.9, respectively. In any case, the little groups of the mentioned points U , S , and R comprise the whole space groups $Pnma$ and $Pbam$, respectively.

Consequently, an antiferromagnetic structure with the magnetic groups

$$M_{62} = Pnma + \{K|0\frac{\bar{1}}{2}\frac{1}{2}\}Pnma \quad (12)$$

and

$$M_{55} = Pbam + \{K|\frac{\bar{1}}{2}10\}Pbam \quad (13)$$

can be stable in $BaFe_2As_2$.

These two magnetic groups M_{62} (12) and M_{55} (13) may be realized by the displacement of the Fe atoms as depicted in Figs. 1 (c) and (d). By means of the generating elements (10) and (11) we may verify that the symmetry operations of the space groups $Pnma$ and $Pbam$ leave these displacements of the Fe atoms invariant. In addition, the displacements of the Fe atoms are also invariant under the anti-unitary operations $\{K|0\frac{\bar{1}}{2}\frac{1}{2}\}$ and $\{K|\frac{\bar{1}}{2}10\}$, respectively, since they connect in any case two atoms with antiparallel magnetic moments and the same displacement.

Consequently, the displacement of the Fe atoms depicted in Figs. 1 (c) and (d) stabilize the experimentally observed antiferromagnetic structure in $BaFe_2As_2$.

V. SUMMARY

In Secs. II and III of this paper we could substantiate the existence of a magnetic band in the band struc-

ture of $BaFe_2As_2$ which is related to the magnetic group M_{64} (2) of the experimentally observed [1] antiferromagnetic state. As described by the nonadiabatic Heisenberg model, the electrons in this extremely narrow and roughly half-filled energy band can lower their Coulomb correlation energy by producing this antiferromagnetic state.

However, this lowering of the energy is forbidden in undistorted $BaFe_2As_2$ because a *stable* antiferromagnetic and its time-inverted state need to form a basis of a suitable irreducible corepresentation of the complete magnetic group of the Hamiltonian. Such a corepresentation is not available in an *undistorted* $BaFe_2As_2$ structure. However, as outlined in Sec. IV.2, a small shift of the Fe positions, brought about by the electron system in the magnetic band, makes the required corepresentation and thus a stable antiferromagnetic state.

We identified in Sec. IV several distortions being able to stabilize the antiferromagnetic state in $BaFe_2As_2$. The two distortions with the highest symmetry are presented in Figs. 1 (c) and (d). They may be realized by the depicted small displacements of the Fe atoms which are invariant under the magnetic groups M_{62} (12) and M_{55} (13), respectively. The related space groups $Pnma$ and $Pbam$ have the same point group D_{2h} as $Cmca$, but a lower translation symmetry: the translation T_1 in Fig. 1 (b) is no longer a lattice translation in the distorted system, see Figs. 1 (c) and (d). We suppose that these two distortions of minor change of the symmetry are energetically more favorable than any other possible distortion of lower symmetry.

ACKNOWLEDGMENTS

We are indebted to Franz-Werner Gergen and Heinz Schühle from the EDV group of the Max-Planck-Institut für Intelligente Systeme and Kilian Krause from the TIK of the University in Stuttgart for their assistance in getting to run the computer programs needed for this work.

-
1. Q. Huang, Y. Qiu, W. Bao, M. A. Green, J. W. Lynn, Y. C. Gasparovic, T. Wu, G. Wu, and X. H. Chen, Phys. Rev. Lett. **101**, 257003 (2008).
 2. E. Krüger, Phys. Rev. B **40**, 11090 (1989).
 3. E. Krüger, Phys. Rev. B **59**, 13795 (1999).
 4. E. Krüger, J. Supercond. **18**(4), 433 (2005).
 5. E. Krüger, Phys. Rev. B **75**, 024408 (2007).
 6. E. Krüger and H. P. Strunk, J. Supercond. **24**, 2103 (2011).
 7. E. Krüger, J. Supercond. **23**, 213 (2010).
 8. E. Krüger and H. P. Strunk, J. Supercond. **25**, 989 (2012).
 9. E. Krüger, Phys. Status Solidi B **85**, 493 (1978).
 10. E. Krüger, J. Supercond. **14**(4), 551 (2001).
 11. E. Krüger, Phys. Rev. B **63**, 144403 (2001).
 12. C. Bradley and A.P. Cracknell, *The Mathematical Theory of Symmetry in Solids* (Clarendon, Oxford, 1972).
 13. V. Blum, R. Gehrke, F. Hanke, P. Havu, V. Havu, X. Ren, K. Reuter, and M. Scheffler, Computer Physics Communications **180**, 2175 (2009).
 14. V. Havu, V. Blum, P. Havu, and M. Scheffler, Computer Physics Communications **228**, 8367 (2009).
 15. E. Krüger, Phys. Rev. B **32**, 7493 (1985).

Appendix: Group-theoretical tables

TABLE A.1. Relationship between the lines of the Brillouin zones for the paramagnetic (Bravais lattice Γ_q^v) and the antiferromagnetic (Bravais lattice Γ_o^b) phases of undistorted BaFe_2As_2 .

$\Delta_M\Gamma, \Delta_MX$	$\Gamma Z, XPX$	ZU_M, XU_M	$\Gamma\Delta X, XYUZ$
$Z\Gamma$	ΓY	$Y\Gamma$	$\Gamma\Delta FY$

Notes to Table A.1

- (i) Always two lines in the paramagnetic Brillouin zone are equivalent to one line in the antiferromagnetic Brillouin zone.
- (ii) The upper row lists pairs of lines in the Brillouin zone for the tetragonal paramagnetic phase. Beneath each pair the equivalent line in the Brillouin zone for the antiferromagnetic structure is listed.
- (iii) The notations of the points and lines of symmetry follow Fig. 3.10. (b) (for Γ_q^v) and Fig. 3.6. (a) (for Γ_o^b) of Ref. [12].
- (iv) XYUZ stands, e.g., for the line between X and Z via the lines Y and U in the Brillouin zone for Γ_q^v , cf. Fig. 2.
- (v) Δ_M and U_M stand for the central points of the lines $\Gamma\Delta X$ and XYUZ, respectively, in the Brillouin zone for Γ_q^v .

TABLE A.2. Character tables of the single-valued irreducible representations of the space group $I4/mmm = \Gamma_q^v D_{4h}^{17}$ (139) of tetragonal paramagnetic BaFe_2As_2 .

$\Gamma(000)$ and $Z(\frac{1}{2}\frac{1}{2}\frac{1}{2})$										$X(00\frac{1}{2})$								$P(\frac{1}{4}\frac{1}{4}\frac{1}{4})$						
										$E C_{2z} C_{2a} C_{2b} I \sigma_z \sigma_{da} \sigma_{db}$								$S_{4z}^- C_{2y} \sigma_{da}$						
										$E C_{2z} C_{4z}^+ C_{2x} C_{2a} I \sigma_z S_{4z}^- \sigma_x \sigma_{da}$								$E C_{2z} S_{4z}^+ C_{2x} \sigma_{db}$						
Γ_1^+, Z_1^+	1	1	1	1	1	1	1	1	1	X_1^+	1	1	1	1	1	1	1	P_1	1	1	1	1	1	
Γ_2^+, Z_2^+	1	1	1	-1	-1	1	1	1	-1	X_2^+	1	-1	1	-1	1	-1	1	-1	P_2	1	1	1	-1	-1
Γ_3^+, Z_3^+	1	1	-1	1	-1	1	1	-1	1	X_3^+	1	1	-1	-1	1	1	-1	-1	P_3	1	1	-1	1	-1
Γ_4^+, Z_4^+	1	1	-1	-1	1	1	1	-1	-1	X_4^+	1	-1	-1	1	1	-1	-1	1	P_4	1	1	-1	-1	1
Γ_5^+, Z_5^+	2	-2	0	0	0	2	-2	0	0	X_1^-	1	1	1	1	-1	-1	-1	-1	P_5	2	-2	0	0	0
Γ_1^-, Z_1^-	1	1	1	1	1	-1	-1	-1	-1	X_2^-	1	-1	1	-1	-1	1	-1	1						
Γ_2^-, Z_2^-	1	1	1	-1	-1	-1	-1	-1	1	X_3^-	1	1	-1	-1	-1	-1	1	1						
Γ_3^-, Z_3^-	1	1	-1	1	-1	-1	-1	1	-1	X_4^-	1	-1	-1	1	-1	1	1	-1						
Γ_4^-, Z_4^-	1	1	-1	-1	1	-1	-1	1	1															
Γ_5^-, Z_5^-	2	-2	0	0	0	-2	2	0	0															

$N(0\frac{1}{2}0)$				
$E C_{2y} I \sigma_y$				
N_1^+	1	1	1	1
N_1^-	1	1	-1	-1
N_2^+	1	-1	1	-1
N_2^-	1	-1	-1	1

Notes to Table A.2

- (i) The space group $I4/mmm$ is symmorphic. Thus, the point group operations alone are symmetry operations.
- (ii) The point group operations are related to the x, y, z coordinates in Fig. 1 (a).
- (iii) The notations of the points of symmetry follow Fig. 3.10. (b) of Ref. [12].
- (iv) The character table is determined from Table 5.7 of Ref. [12].

TABLE A.3. Compatibility relations between points and lines in the Brillouin zone for tetragonal paramagnetic BaFe₂As₂ (space group $I4/mmm$).

$\Gamma(000)$										$X(00\frac{1}{2})$							
Γ_1^+	Γ_2^+	Γ_3^+	Γ_4^+	Γ_5^+	Γ_1^-	Γ_2^-	Γ_3^-	Γ_4^-	Γ_5^-	X_1^+	X_2^+	X_3^+	X_4^+	X_1^-	X_2^-	X_3^-	X_4^-
Δ_1	Δ_2	Δ_2	Δ_1	$\Delta_3 + \Delta_4$	Δ_3	Δ_4	Δ_4	Δ_3	$\Delta_1 + \Delta_2$	Δ_1	Δ_3	Δ_2	Δ_4	Δ_3	Δ_1	Δ_4	Δ_2
$Z(\frac{1}{2}\frac{1}{2}\frac{1}{2})$										$X'(\frac{1}{2}\frac{1}{2}0)$							
Z_1^+	Z_2^+	Z_3^+	Z_4^+	Z_5^+	Z_1^-	Z_2^-	Z_3^-	Z_4^-	Z_5^-	X_1^+	X_2^+	X_3^+	X_4^+	X_1^-	X_2^-	X_3^-	X_4^-
U_1	U_2	U_2	U_1	$U_3 + U_4$	U_3	U_4	U_4	U_3	$U_1 + U_2$	Y_1	Y_4	Y_2	Y_3	Y_3	Y_2	Y_4	Y_1

Notes to Table A.3

- (i) The notations of the points and lines of symmetry follow Fig. 3.10. (b) of Ref. [12].
- (ii) $Z(\frac{1}{2}\frac{1}{2}\frac{1}{2})$ and $X'(\frac{1}{2}\frac{1}{2}0)$ are connected via the lines U and Y . The symmetry labels are chosen in such a way that $U_i = Y_i$ (for $i = 1, 2, 3, 4$).
- (iii) This table defines the labels Δ_i and U_i which are needed in Table A.5 to find the representations of the magnetic band at Z and T .

TABLE A.4. Character tables of the single-valued irreducible representations of the orthorhombic space group $Cmca = \Gamma_o D_{2h}^{18}$ (64) of the experimentally observed [1] antiferromagnetic structure depicted in Fig. 1 (b).

$\Gamma(000)$ and $Y(\frac{1}{2}\frac{1}{2}0)$										
	$\{E 000\}$	$\{C_{2b} \frac{1}{2}\frac{1}{2}\frac{1}{2}\}$	$\{C_{2a} \frac{1}{2}\frac{1}{2}\frac{1}{2}\}$	$\{C_{2z} 000\}$	$\{I 000\}$	$\{\sigma_{db} \frac{1}{2}\frac{1}{2}\frac{1}{2}\}$	$\{\sigma_{da} \frac{1}{2}\frac{1}{2}\frac{1}{2}\}$	$\{\sigma_z 000\}$		
Γ_1^+, Y_1^+	1	1	1	1	1	1	1	1	1	1
Γ_2^+, Y_2^+	1	-1	1	-1	1	-1	1	-1	-1	-1
Γ_3^+, Y_3^+	1	1	-1	-1	1	1	-1	-1	-1	-1
Γ_4^+, Y_4^+	1	-1	-1	1	1	-1	-1	-1	1	1
Γ_1^-, Y_1^-	1	1	1	1	-1	-1	-1	-1	-1	-1
Γ_2^-, Y_2^-	1	-1	1	-1	-1	1	-1	-1	1	1
Γ_3^-, Y_3^-	1	1	-1	-1	-1	-1	-1	1	1	1
Γ_4^-, Y_4^-	1	-1	-1	1	-1	1	1	1	-1	-1

$Z(00\frac{1}{2})$ and $T(\frac{1}{2}\frac{1}{2}\frac{1}{2})$										
	$\{E 000\}$	$\{E 001\}$	$\{C_{2b} \frac{1}{2}\frac{1}{2}\frac{3}{2}\}$	$\{I 001\}$	$\{\sigma_{db} \frac{1}{2}\frac{1}{2}\frac{3}{2}\}$	$\{\sigma_{da} \frac{1}{2}\frac{1}{2}\frac{3}{2}\}$	$\{C_{2z} 001\}$	$\{C_{2a} \frac{1}{2}\frac{1}{2}\frac{3}{2}\}$		
Z_1, T_1	2	-2	0	0	0	2	-2	0	0	0
Z_2, T_2	2	-2	0	0	0	-2	2	0	0	0

$R(0\frac{1}{2}\frac{1}{2})$										
	K	$\{K \frac{1}{2}\frac{1}{2}\frac{1}{2}\}$	$\{E 000\}$	$\{\sigma_{db} \frac{1}{2}\frac{1}{2}\frac{1}{2}\}$	$\{E 001\}$	$\{\sigma_{db} \frac{1}{2}\frac{1}{2}\frac{3}{2}\}$	$\{I 001\}$	$\{C_{2b} \frac{1}{2}\frac{1}{2}\frac{3}{2}\}$	$\{I 000\}$	$\{C_{2b} \frac{1}{2}\frac{1}{2}\frac{1}{2}\}$
R_1^+ (c)	(a)	1	i	-1	-i	1	i	-1	-i	-i
R_2^+ (c)	(a)	1	-i	-1	i	1	-i	-1	i	i
R_1^- (c)	(a)	1	i	-1	-i	-1	-i	1	1	i
R_2^- (c)	(a)	1	-i	-1	i	-1	i	1	1	-i

Notes to Table A.4

- (i) The notations of the points of symmetry follow Fig. 3.6. (a) of Ref. [12].
- (ii) Point S is not listed because it has only one two-dimensional representation S_1 irrelevant in this paper.
- (iii) The space group operations are related to the coordinate system in Fig. 1 (b).
- (iv) The character tables are determined from Table 5.7 in Ref. [12]. The origin of the coordinate system used in Ref. [12] for $Cmca$ is translated into the origin used in this paper by $\mathbf{t}_0 = \frac{1}{4}\mathbf{T}_1 + \frac{1}{4}\mathbf{T}_2$. Thus, the symmetry operations P_{bc} given in Table 5.7 of Ref. [12] are changed into the operations P_p used in this paper by the equation

$$P_p = \{E|\mathbf{t}_0\}P_{bc}\{E|-\mathbf{t}_0\},$$

where E is the identity operation.

- (v) The cases (a) and (c) are defined in equations (7.3.45) and (7.3.47), respectively, of Ref. [12] and are determined by equation (7.3.51) of Ref. [12].

TABLE A.5. Compatibility relations between the Brillouin zone for tetragonal paramagnetic BaFe₂As₂ and the Brillouin zone for the orthorhombic antiferromagnetic structure depicted in Figs. 1 (a) and (b), respectively.

$\Gamma(000)$										$X(00\frac{1}{2})$														
Γ_1^+	Γ_2^+	Γ_3^+	Γ_4^+	Γ_5^+	Γ_1^-	Γ_2^-	Γ_3^-	Γ_4^-	Γ_5^-	X_1^+	X_2^+	X_3^+	X_4^+	X_1^-	X_2^-	X_3^-	X_4^-							
Γ_1^+	Γ_4^+	Γ_4^+	Γ_1^+	Γ_2^+	Γ_3^+	Γ_1^-	Γ_4^-	Γ_4^-	Γ_1^-	Γ_2^-	Γ_3^-	Γ_4^-	Γ_1^-	Γ_2^-	Γ_3^-	Γ_4^-	Y_1^+	Y_2^+	Y_4^+	Y_3^+	Y_1^-	Y_2^-	Y_4^-	Y_3^-
$Z(\frac{1}{2}\frac{1}{2}\frac{1}{2})$										$X'(\frac{1}{2}\frac{1}{2}0)$														
Z_1^+	Z_2^+	Z_3^+	Z_4^+	Z_5^+	Z_1^-	Z_2^-	Z_3^-	Z_4^-	Z_5^-	X_1^+	X_2^+	X_3^+	X_4^+	X_1^-	X_2^-	X_3^-	X_4^-							
Y_4^+	Y_1^+	Y_1^+	Y_4^+	Y_2^+	Y_3^+	Y_4^-	Y_1^-	Y_1^-	Y_4^-	Y_2^-	Y_3^-	Γ_4^+	Γ_2^+	Γ_1^+	Γ_3^+	Γ_4^-	Γ_2^-	Γ_1^-	Γ_3^-					
$N'(\frac{1}{2}0\frac{1}{2})$				$\Delta'_M(\frac{1}{4}\frac{1}{4}0)$				$U'_M(\frac{3}{4}\frac{1}{4}\frac{1}{2})$																
N_1^+	N_1^-	N_2^+	N_2^-	Δ_1	Δ_3	Δ_2	Δ_4	U_1	U_3	U_2	U_4													
$R_1^- + R_2^-$	$R_1^+ + R_2^+$	$R_1^- + R_2^-$	$R_1^+ + R_2^+$	Z_1	Z_2	Z_1	Z_2	T_1	T_2	T_1	T_2													

Notes to Table A.5

- (i) The antiferromagnetic structure in Fig. 1 (b) has the space group $Cmca$.
- (ii) The Brillouin zone for the orthorhombic space group $Cmca$ lies within the Brillouin zone for the tetragonal space group $I4/mmm$.
- (iii) $\Delta_M(00\frac{1}{4})$ and $U_M(\frac{1}{2}\frac{1}{2}\frac{1}{4})$ stand for the central points of the lines connecting Γ with $X(00\frac{1}{2})$ and $Z(\frac{1}{2}\frac{1}{2}\frac{1}{2})$ with $X'(\frac{1}{2}\frac{1}{2}0)$, respectively.
- (iv) The points X' , N' , Δ'_M , and U'_M do not belong to the basic domain of the Brillouin zone but can be generated by the action of the point group operations C_{4z}^+ , C_{2z} , C_{4z}^+ , and C_{4z}^+ on X , N , Δ_M , and U_M , respectively.
- (v) The upper rows list the representations of the little groups of the points of symmetry in the Brillouin zone for the tetragonal paramagnetic phase. The lower rows list representations of the little groups of the related points of symmetry in the Brillouin zone for the antiferromagnetic structure.
The representations in the same column are compatible in the following sense: Bloch functions that are basis functions of a representation D_i in the upper row can be unitarily transformed into the basis functions of the representation given below D_i .
- (vi) The symmetry labels for the points of symmetry are given in Tables A.2 and A.4, respectively.
- (vii) The symmetry labels for the lines Δ and U are defined by Table A.3.
- (viii) The compatibility relations are determined in the way described in great detail in Ref. [15].

TABLE A.6. Compatibility relations between the points $\Gamma(000)$ and $Y(\frac{\bar{1}}{2}\frac{1}{2}0)$ and the line connecting these points in the Brillouin zone for the antiferromagnetic structure in undistorted BaFe_2As_2 (space group $Cmca$).

$\Gamma(000)$								$Y(\frac{\bar{1}}{2}\frac{1}{2}0)$							
Γ_1^+	Γ_2^+	Γ_3^+	Γ_4^+	Γ_1^-	Γ_2^-	Γ_3^-	Γ_4^-	Y_1^+	Y_2^+	Y_3^+	Y_4^+	Y_1^-	Y_2^-	Y_3^-	Y_4^-
Δ_1	Δ_3	Δ_4	Δ_2	Δ_3	Δ_1	Δ_2	Δ_4	F_1	F_3	F_4	F_2	F_3	F_1	F_2	F_4

Notes to Table A.6

- (i) The notations of the points and lines of symmetry follow Fig. 3.6. (a) of Ref. [12].
- (ii) $\Gamma(000)$ and $Y(\frac{\bar{1}}{2}\frac{1}{2}0)$ are connected via the lines Δ and F . The symmetry notations are chosen in such a way that $\Delta_i = F_i$ (for $i = 1, 2, 3, 4$).
- (iii) This table defines the labels Δ_i and F_i which are needed to construct the magnetic band between $\Gamma(000)$ and $Y(\frac{\bar{1}}{2}\frac{1}{2}0)$ in Fig. 3.

TABLE A.7. Single-valued representations of all the energy bands of antiferromagnetic BaFe_2As_2 with symmetry-adapted and optimally localized Wannier functions centered at the Fe atoms.

Fe	Γ	Y	Z	T	R
Band 1	$\Gamma_1^+ + \Gamma_2^+ + \Gamma_1^- + \Gamma_2^-$	$Y_1^+ + Y_2^+ + Y_1^- + Y_2^-$	$Z_1 + Z_2$	$T_1 + T_2$	$R_1^+ + R_2^+ + R_1^- + R_2^-$
Band 2	$\Gamma_3^+ + \Gamma_4^+ + \Gamma_3^- + \Gamma_4^-$	$Y_3^+ + Y_4^+ + Y_3^- + Y_4^-$	$Z_1 + Z_2$	$T_1 + T_2$	$R_1^+ + R_2^+ + R_1^- + R_2^-$

Notes to Table A.7

- (i) The antiferromagnetic structure of undistorted BaFe_2As_2 depicted in Fig. 1 (b) has the space group $Cmca$ and the magnetic group $M = Cmca + \{K|\frac{\bar{1}}{2}\frac{1}{2}\frac{1}{2}\}Cmca$ with K denoting the operator of time-inversion.
- (ii) The two listed bands form “magnetic bands” related to M .
- (iii) Each row defines one band consisting of four branches, because there are four Fe atoms in the unit cell.
- (iv) The representations are given in Table A.4.
- (v) The bands are determined by Eq. (23) of Ref. [4].
- (vi) Assume the tetragonal band structure of BaFe_2As_2 to be folded into the Brillouin zone for the antiferromagnetic phase (as carried out in Fig. 3) and assume further a band of the symmetry in any row of this table to exist in the folded band structure. Then the Bloch functions of this band can be unitarily transformed into Wannier functions that are
 - as well localized as possible;
 - centered at the Fe atoms;
 - and symmetry-adapted to the space group $Cmca$ of the antiferromagnetic phase.
- (vii) Eq. (23) of Ref. [4] makes sure that the Wannier function may be chosen to be symmetry-adapted to the *space* group

$Cmca$ of the antiferromagnetic phase. In addition, there exists a Matrix \mathbf{N} , namely $\mathbf{N} = \begin{pmatrix} 0 & 0 & 1 & 0 \\ 0 & 0 & 0 & 1 \\ 1 & 0 & 0 & 0 \\ 0 & 1 & 0 & 0 \end{pmatrix}$, satisfying both

Eqs. (26) (with $\{K|\frac{\bar{1}}{2}\frac{1}{2}\frac{1}{2}\}$) and (32) of Ref. [4] for the two bands listed in this table. Hence, the Wannier functions may be chosen symmetry adapted to the magnetic group $M = Cmca + \{K|\frac{\bar{1}}{2}\frac{1}{2}\frac{1}{2}\}Cmca$.

TABLE A.8. Character tables of the single-valued irreducible representations of the orthorhombic space group $Pnma = \Gamma_o D_{2h}^{16}$ (62).

		$U(0\frac{1}{2}\frac{1}{2})$							
K		$\{K 0\frac{1}{2}\frac{1}{2}\}$	$\{E 000\}$	$\{C_{2a} 0\frac{1}{2}\frac{1}{2}\}$	$\{E 001\}$	$\{C_{2a} 0\frac{1}{2}\frac{3}{2}\}$	$\{C_{2z} 0\frac{1}{2}0\}$	$\{C_{2b} 0\frac{1}{2}0\frac{3}{2}\}$	$\{C_{2z} 0\frac{1}{2}1\}$
U_1^-	(c) (a)	1	i	-1	-i	1	i	-1	-1
U_2^-	(c) (a)	1	-i	-1	i	1	-i	-1	-1
U_3^-	(c) (a)	1	i	-1	-i	-1	-i	1	1
U_4^-	(c) (a)	1	-i	-1	i	-1	i	1	1
U_1^+	(c) (a)	1	i	-1	-i	1	i	-1	-1
U_2^+	(c) (a)	1	-i	-1	i	1	-i	-1	-1
U_3^+	(c) (a)	1	i	-1	-i	-1	-i	1	1
U_4^+	(c) (a)	1	-i	-1	i	-1	i	1	1

		$U(0\frac{1}{2}\frac{1}{2})$ (continued)								
		$\{C_{2b} 0\frac{1}{2}0\frac{1}{2}\}$	$\{I 0\frac{1}{2}0\}$	$\{\sigma_{da} 0\frac{1}{2}0\frac{3}{2}\}$	$\{I 0\frac{1}{2}1\}$	$\{\sigma_{da} 0\frac{1}{2}0\frac{1}{2}\}$	$\{\sigma_z 000\}$	$\{\sigma_{db} 0\frac{1}{2}0\frac{1}{2}\}$	$\{\sigma_z 001\}$	$\{\sigma_{db} 0\frac{1}{2}0\frac{3}{2}\}$
U_1^-	-i	1	i	-1	-i	1	i	-1	-i	
U_2^-	i	1	-i	-1	i	1	-i	-1	i	
U_3^-	i	1	i	-1	-i	-1	-i	1	i	
U_4^-	-i	1	-i	-1	i	-1	i	1	-i	
U_1^+	-i	-1	-i	1	i	-1	-i	1	i	
U_2^+	i	-1	i	1	-i	-1	i	1	-i	
U_3^+	i	-1	-i	1	i	1	i	-1	-i	
U_4^+	-i	-1	i	1	-i	1	-i	-1	i	

Notes to Table A.8

- (i) The notations of the points of symmetry follow Fig. 3.5. of Ref. [12].
- (ii) Only the listed point U is relevant in this paper.
- (iii) The notation of the space group operations is related to the coordinate system in Fig. 1 (c).
- (iv) The character tables are determined from Table 5.7 in Ref. [12]. The origin of the coordinate system used in Ref. [12] for $Pnma$ is identical with the origin used in this paper.
- (v) The cases (a) and (c) are defined in equations (7.3.45) and (7.3.47), respectively, of Ref. [12] and are determined by equation (7.3.51) of Ref. [12]

TABLE A.9. Character tables of the single-valued irreducible representations of the orthorhombic space group $Pbam = \Gamma_o D_{2h}^9$ (55).

		$S(\overline{1}\frac{1}{2}0)$							
K	$\{K \overline{1}\frac{1}{2}0\}$	$\{E 000\}$	$\{C_{2b} \frac{1}{2}\frac{1}{2}0\}$	$\{E 010\}$	$\{C_{2b} \frac{1}{2}\frac{3}{2}0\}$	$\{C_{2z} 000\}$	$\{C_{2a} \frac{1}{2}\frac{1}{2}0\}$	$\{C_{2z} 010\}$	
S_1^-	(c)	(a)	1	i	-1	-i	1	i	-1
S_2^-	(c)	(a)	1	-i	-1	i	1	-i	-1
S_3^-	(c)	(a)	1	i	-1	-i	-1	-i	1
S_4^-	(c)	(a)	1	-i	-1	i	-1	i	1
S_1^+	(c)	(a)	1	i	-1	-i	1	i	-1
S_2^+	(c)	(a)	1	-i	-1	i	1	-i	-1
S_3^+	(c)	(a)	1	i	-1	-i	-1	-i	1
S_4^+	(c)	(a)	1	-i	-1	i	-1	i	1

		$S(\overline{1}\frac{1}{2}0)$ (continued)							
	$\{C_{2a} \frac{1}{2}\frac{3}{2}0\}$	$\{I 000\}$	$\{\sigma_{db} \frac{1}{2}\frac{1}{2}0\}$	$\{I 010\}$	$\{\sigma_{db} \frac{1}{2}\frac{3}{2}0\}$	$\{\sigma_z 000\}$	$\{\sigma_{da} \frac{1}{2}\frac{1}{2}0\}$	$\{\sigma_z 010\}$	$\{\sigma_{da} \frac{1}{2}\frac{3}{2}0\}$
S_1^-	-i	1	i	-1	-i	1	i	-1	-i
S_2^-	i	1	-i	-1	i	1	-i	-1	i
S_3^-	i	1	i	-1	-i	-1	-i	1	i
S_4^-	-i	1	-i	-1	i	-1	i	1	-i
S_1^+	-i	-1	-i	1	i	-1	-i	1	i
S_2^+	i	-1	i	1	-i	-1	i	1	-i
S_3^+	i	-1	-i	1	i	1	i	-1	-i
S_4^+	-i	-1	i	1	-i	1	-i	-1	i

		$R(\overline{1}\frac{1}{2}\frac{1}{2})$							
K	$\{K \overline{1}\frac{1}{2}\frac{1}{2}\}$	$\{E 000\}$	$\{C_{2b} \frac{1}{2}\frac{1}{2}0\}$	$\{E 001\}$	$\{C_{2b} \frac{1}{2}\frac{1}{2}1\}$	$\{C_{2z} 000\}$	$\{C_{2a} \frac{1}{2}\frac{1}{2}0\}$	$\{C_{2z} 001\}$	
R_1^-	(c)	(a)	1	i	-1	-i	1	i	-1
R_2^-	(c)	(a)	1	-i	-1	i	1	-i	-1
R_3^-	(c)	(a)	1	i	-1	-i	-1	-i	1
R_4^-	(c)	(a)	1	-i	-1	i	-1	i	1
R_1^+	(c)	(a)	1	i	-1	-i	1	i	-1
R_2^+	(c)	(a)	1	-i	-1	i	1	-i	-1
R_3^+	(c)	(a)	1	i	-1	-i	-1	-i	1
R_4^+	(c)	(a)	1	-i	-1	i	-1	i	1

		$R(\overline{1}\frac{1}{2}\frac{1}{2})$ (continued)							
	$\{C_{2a} \frac{1}{2}\frac{1}{2}1\}$	$\{I 000\}$	$\{\sigma_{db} \frac{1}{2}\frac{1}{2}0\}$	$\{I 001\}$	$\{\sigma_{db} \frac{1}{2}\frac{1}{2}1\}$	$\{\sigma_z 000\}$	$\{\sigma_{da} \frac{1}{2}\frac{1}{2}0\}$	$\{\sigma_z 001\}$	$\{\sigma_{da} \frac{1}{2}\frac{1}{2}1\}$
R_1^-	-i	1	i	-1	-i	1	i	-1	-i
R_2^-	i	1	-i	-1	i	1	-i	-1	i
R_3^-	i	1	i	-1	-i	-1	-i	1	i
R_4^-	-i	1	-i	-1	i	-1	i	1	-i
R_1^+	-i	-1	-i	1	i	-1	-i	1	i
R_2^+	i	-1	i	1	-i	-1	i	1	-i
R_3^+	i	-1	-i	1	i	1	i	-1	-i
R_4^+	-i	-1	i	1	-i	1	-i	-1	i

Notes to Table A.9

- (i) The notations of the points of symmetry follow Fig. 3.5. of Ref. [12].
- (ii) Only the listed points S and R are relevant in this paper.
- (iii) The notation of the space group operations is related to the coordinate system in Fig. 1 (d).
- (iv) The character tables are determined from Table 5.7 in Ref. [12]. The origin of the coordinate system used in Ref. [12] for $Pbam$ is identical with the origin used in this paper.
- (v) The cases (a) and (c) are defined in equations (7.3.45) and (7.3.47), respectively, of Ref. [12] and are determined by equation (7.3.51) of Ref. [12].